IOPscience iopscience.iop.org

Home Search Collections Journals About Contact us My IOPscience

The effects of noise on iterated maps

This article has been downloaded from IOPscience. Please scroll down to see the full text article.

1985 J. Phys. A: Math. Gen. 18 1457

(http://iopscience.iop.org/0305-4470/18/9/026)

View the table of contents for this issue, or go to the journal homepage for more

Download details:
IP Address: 129.252.86.83
The article was downloaded on 31/05/2010 at 09:54

Please note that terms and conditions apply.

J. Phys. A: Math. Gen. **18** (1985) 1457-1474. Printed in Great Britain

The effects of noise on iterated maps

J M Deutsch†

Cavendish Laboratory, Madingley Road, Cambridge CB3 OHE, UK

Received 31 August 1984, in final form 28 November 1984

Abstract. The properties of a simple one-dimensional iterated map in the presence of noise are examined. It is demonstrated that there are three distinct classes of noise that generate three 'phases' of the iterated function. Each phase shows universal properties that are independent of the specific form of noise, if this noise is chosen from a given class. The physical interpretation of the model in terms of aggregation is discussed.

1. Introduction

The effects of noise on iterative maps have been extensively investigated in recent years (Huberman and Rudnick 1980, Shraiman *et al* 1981, Crutchfield *et al* 1981, Hirsch *et al* 1982, Feigenbaum and Hasslacher 1982). This work has concentrated on the effects of noise on the transition to chaos. For example, the one-dimensional map (Feigenbaum 1978) of the form $x_{i+1} = h(x_i) + \xi_i$, where $h(x)$ is a continuous function with a parabolic maximum and ξ_i is a random variable, has a Lyapanov characteristic exponent which has been shown to satisfy scaling laws near the transition to chaos. Another functional form (Geisel and Nierwetberg 1982) of $h(x) = x - \mu \sin(2\pi x)$, leads to the onset of deterministic diffusion as the parameter μ is varied. In the presence of noise it was shown that the diffusion coefficient satisfies universal scaling laws near the transition to diffusion.

Here we find transitions induced by noise in iterative maps with properties that are very different from others previously studied (a brief account of some of the results found here is given in Deutsch (1984)). To illustrate the nature of these transitions we consider a particularly simple map where exact results are obtained; we study the effects of random noise on iterations of $h(x) = x$, corresponding to the case $\mu = 0$ in Geisel and Nierwetberg's work. The properties of this function as it is iterated are trivial. However, the introduction of noise induces large changes in functional behaviour as the number of iterations go to infinity. A major difference between this and previous work is that in the present work there is no transition in functional behaviour in the absence of noise. Also the properties described here involve the entire iterated function, whereas previous work has concentrated on the iterated function evaluated at some arbitrary point. We will show that it is possible to define 'order parameters' for the different 'phases' that the map is in. Each 'phase' of the map corresponds to the particular class of functions that are accessible by iteration (i.e. have non-zero measure in the ensemble of the added noise). Which phase the map is in is determined by the type of noise that is added. It is surprising to note that the transition between different phases is accompanied by non-analytic behaviour only for

† Present address: Institute for Theoretical Physics, University of California, Santa Barbara, California 93106, USA.

0305-4470/85/091457+18$02.25 © 1985 The Institute of Physics

some ensembled averaged quantities, and not for others. In fact, it is the probability distribution of derivatives of the iterated function, and not the probability distribution of the function at a given point, that determines the order parameter for the system.

2. The model

The iterative map $g_n(x)$ examined here is of the form

$$g_n(x) = f_n(f_{n-1}(\ldots(f_1(x))\ldots)) \tag{1}$$

where

$$f_i(x) = x + \varepsilon_i(x) \tag{2}$$

and $\varepsilon_i(x)$ is a random function that is continuous and differentiable, whose statistical properties are independent of x. That is, for a general functional Γ and for all x_0

$$\langle \Gamma(\varepsilon_i(x)) \rangle = \langle \Gamma(\varepsilon_i(x + x_0)) \rangle. \tag{3}$$

Here the average $\langle \ldots \rangle$ is taken over the probability distribution of $\varepsilon_i(x)$. Every random function ε_i with subscript i is statistically independent of all other random functions with different subscripts. For simplicity, we set $\langle \varepsilon_i(x) \rangle = 0$.

Since the properties of the noise are translationally invariant, the statistical properties of $(g_n(x) - x)$ should also be translationally invariant, since for a general functional

$$\begin{aligned} \langle \Gamma(g_n(x) - x) \rangle &= \langle \Gamma(\varepsilon_1(x + \varepsilon_2(x + \cdots))) \rangle \\ &= \langle \Gamma(\varepsilon_1(x + x_0 + \varepsilon_2(x + x_0 + \cdots))) \rangle \\ &= \langle \Gamma(g_n(x + x_0) - (x + x_0)) \rangle \end{aligned} \tag{4}$$

for all x_0. There is also a dilation symmetry whereby the noise amplitude can be scaled down, with a corresponding increase in spatial frequency, i.e. if $x \to x/a$ and $\varepsilon_i(x) \to a\varepsilon_i(x/a)$ then $g_n(x) \to a g_n(x/a)$. This observation implies that we can choose the amplitude of the noise to be arbitrarily small and still maintain the same spatial properties as in the case of high amplitude noise, as long as we rescale the x axis accordingly. If there are different phases, depending on the type of added noise, the amplitude of the noise by itself cannot determine which phase the map is in. There must be dependence on spatial characteristics as well. We will see what quantities are relevant to the transitions in the next section.

3. Calculations

In order to understand the behaviour of $g_n(x)$, we now calculate some simple averages.

The probability of $g_n(x)$ taking a value a, at point x, is simply

$$\begin{aligned} P_n(a; x) &= \langle \delta(g_n(x) - a) \rangle \\ &= \int\int \delta(y + \varepsilon(y) - a) P_{n-1}(y; x) P(\varepsilon)\, \mathrm{d}y\, \mathrm{d}\varepsilon \\ &= \int P_{n-1}(a - \varepsilon; x) P(\varepsilon)\, \mathrm{d}\varepsilon \end{aligned} \tag{5}$$

where $P(\varepsilon)$ is the probability of the noise taking a value ε. Thus $P_n(a;x)$ is the probability distribution for a random walk that starts at point x, i.e. for large n

$$P_n(a;x)=\frac{1}{(2\pi)^{1/2}\sigma_n}\exp\left(-\frac{(a-x)^2}{2\sigma_n^2}\right) \tag{6}$$

with $\sigma_n=n\langle\varepsilon^2\rangle$. It is clear that this distribution shows no change in analytic structure as the type of noise ($P(\varepsilon)$) is varied. It is shown below, however, that the probability distribution for the derivatives of g_n, $p_n(a)$, does show a change in analytic structure as the probability distribution for the derivatives of $f(x)$, $p(a)$, is varied. The equation for $p_n(a)$ is

$$\begin{aligned}p_n(a)&=\langle\delta(g_n'(x)-a)\rangle\\&=\langle\delta(f_n'(g_{n-1}(x))g_{n-1}'(x)-a)\rangle\\&=\int p\left(\frac{a}{w}\right)p_{n-1}(w)\frac{\mathrm{d}w}{|w|}.\end{aligned} \tag{7}$$

To solve this equation, separate the integral into positive and negative regions of integration:

$$p_n(a)=\int_0^\infty\left[p\left(\frac{a}{w}\right)p_{n-1}(w)+p\left(-\frac{a}{w}\right)p_{n-1}(-w)\right]\frac{\mathrm{d}w}{w} \tag{8}$$

and define $\mathrm{e}^y=w$, $u_n(y)=p_n(\mathrm{e}^y)$ and $v_n(y)=p_n(-\mathrm{e}^y)$. Then for $a>0$

$$u_n(\ln a)=\int_{-\infty}^\infty u(\ln a-y)u_{n-1}(y)\,\mathrm{d}y+\int_{-\infty}^\infty v(\ln a-y)v_{n-1}(y)\,\mathrm{d}y \tag{9}$$

and for $a<0$

$$v_n(\ln(-a))=\int_{-\infty}^\infty v(\ln(-a)-y)u_{n-1}(y)\,\mathrm{d}y+\int_{-\infty}^\infty u(\ln(-a)-y)v_{n-1}(y)\,\mathrm{d}y. \tag{10}$$

We now introduce the two-sided Laplace transforms

$$\begin{aligned}\hat{u}_n(s)&=\int_{-\infty}^\infty u_n(x)\,\mathrm{e}^{sx}\,\mathrm{d}x\\\hat{v}_n(s)&=\int_{-\infty}^\infty v_n(x)\,\mathrm{e}^{sx}\,\mathrm{d}x.\end{aligned} \tag{11}$$

It what follows, we shall assume for simplicity that these are defined in the range $-\infty<s<\infty$. However the results can be trivially generalised to the case where $\hat{u}_n(s)$ and $\hat{v}_n(s)$ are only defined on the interval $s_l<s<s_u$, where s_l is less than one and s_u is greater than one. This corresponds to the restriction on p that

$$\lim_{|x|\to 0}p(x)<|x|^\alpha$$

where $\alpha>-1$, and

$$\lim_{|x|\to\infty}p(x)<x^\beta$$

where $\beta < -1$. Therefore (10) becomes

$$\begin{aligned} \hat{u}_n(s) &= \hat{u}(s)\hat{u}_{n-1}(s) + \hat{v}(s)\hat{v}_{n-1}(s) \\ \hat{v}_n(s) &= \hat{v}(s)\hat{u}_{n-1}(s) + \hat{u}(s)\hat{v}_{n-1}(s). \end{aligned} \tag{12}$$

Adding and subtracting these the equations gives

$$\begin{aligned} \hat{u}_n(s) + \hat{v}(s) &= (\hat{u}(s) + \hat{v}(s))^n \\ \hat{u}_n(s) - \hat{v}(s) &= (\hat{u}(s) - \hat{v}(s))^n. \end{aligned} \tag{13}$$

So we obtain the solution equation (7)

$$\hat{u}_n(s) = \tfrac{1}{2}[(\hat{u}(s) + \hat{v}(s))^n + (\hat{u}(s) - \hat{v}(s))^n] \tag{14a}$$

$$\hat{v}_n(s) = \tfrac{1}{2}[(\hat{u}(s) + \hat{v}(s))^n - (\hat{u}(s) - \hat{v}(s))^n]. \tag{14b}$$

Now we discuss some general properties of $u_n(s)$. Because $u_n(x)$, $v_n(x) > 0$, $\hat{u}_n(s)$, $\hat{v}_n(s) > 0$. Since

$$\int p_n(w)\, \mathrm{d}w = 1 \tag{15a}$$

$$\int w p_n(w)\, \mathrm{d}w = 1 \tag{15b}$$

then for any distribution other than the trivial case $p_n(w) = \delta(w-1)$, $\lim_{s \to \pm\infty} \hat{u}_n = \infty$. Furthermore, it is easy to show that both the functions $\hat{u}_n(s)$ and $\hat{u}_n(s) + \hat{v}_n(s)$ have only one minimum. This will be shown for $\hat{u}_n(s)$. The proof for the case of $\hat{u}_n(s) + \hat{v}_n(s)$ is identical. If we assume the converse, that there are two minima at s_1 and s_2, then

$$\frac{\mathrm{d}}{\mathrm{d}s}\, \hat{u}_n(s)\bigg|_{s=s_1,s_2} = \int_{-\infty}^{\infty} y\, \mathrm{e}^{sy} u_n(y)\, \mathrm{d}y \bigg|_{s=s_1,s_2} = 0. \tag{16}$$

Define

$$\begin{aligned} I_1^+ &= \int_0^{\infty} y\, \mathrm{e}^{s_1 y} u_n(y)\, \mathrm{d}y \\ I_2^+ &= \int_0^{\infty} y\, \mathrm{e}^{s_2 y} u_n(y)\, \mathrm{d}y \\ I_1^- &= -\int_{-\infty}^{0} y\, \mathrm{e}^{s_1 y} u_n(y)\, \mathrm{d}y \\ I_2^- &= -\int_{-\infty}^{0} y\, \mathrm{e}^{s_2 y} u_n(y)\, \mathrm{d}y \end{aligned} \tag{17}$$

so with the convention that $s_2 > s_1$ we have

$$I_2^+ > I_1^+, \qquad I_2^- < I_1^- \tag{18}$$

but by equation (16), $I_2^+ = I_2^-$ and $I_1^+ = I_1^-$, which implies by equation (18) that $I_2^+ < I_1^+$ which is a contradiction. Therefore there is only one minimum of $\hat{u}_n(s)$.

We now discuss the case where $v(x) = 0$ for all x. We label this regime 1. This corresponds to the case where the functions $f_i(x)$ are all monotonic. Equation (15) implies that $\hat{u}(1) = \hat{u}(2) = 1$, so that the asymptotic limits of $\hat{u}(s)$, together with the

fact that $u_n(s)$ has only one minimum, implies that $\hat{u}(s) < 1$ for $1 < s < 2$. A sketch of $\hat{u}(s)$ is in figure 1. Therefore $\lim_{n\to\infty} \hat{u}_n(s) = \lim_{n\to\infty} \hat{u}^n(s) = 0$ for $1 < s < 2$.

Define the 'order parameter'

$$O^+ = \lim_{\epsilon\to+0} \lim_{n\to\infty} \int_0^\epsilon p_n(w)\,\mathrm{d}w$$

$$= \lim_{x\to-\infty} \lim_{n\to\infty} \int_{-\infty}^{x} \mathrm{e}^y u_n(y)\,\mathrm{d}y. \tag{19}$$

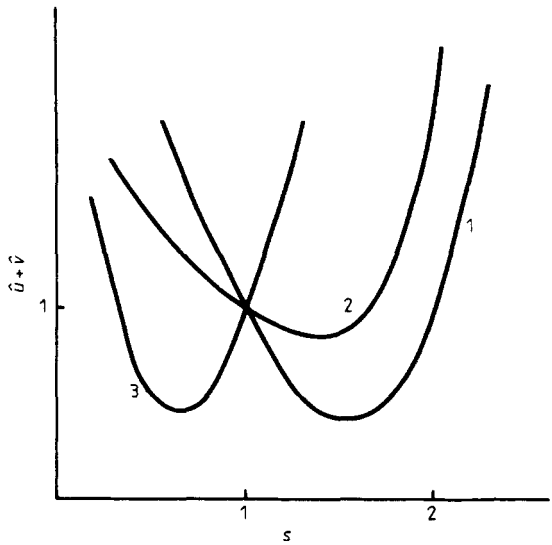

Figure 1. The function $\hat{u}(s)+\hat{v}(s)$ plotted against s as defined by equation (11), sketched in all three regimes. In regime 1, $\hat{u}(1)+\hat{v}(1) = \hat{u}(2)+\hat{v}(2) = 1$ and the minimum of the function is when s is between 1 and 2. In regime 2, the minimum of $\hat{u}(s)+\hat{v}(s)$ is still when s is between 1 and 2, but now $\hat{u}(2)+\hat{v}(2) > 1$. In regime 3, the value of s where the minimum occurs has shifted to less than 1.

By choosing any q such that $0 < q < 1$ we have

$$1 - O^+ = \lim_{x\to-\infty} \lim_{n\to\infty} \int_x^\infty \mathrm{e}^y u_n(y)\,\mathrm{d}y$$

$$\leqslant \lim_{x\to-\infty} \lim_{n\to\infty} \int_{-\infty}^{\infty} \mathrm{e}^{q(y-x)}\,\mathrm{e}^y u_n(y)\,\mathrm{d}y$$

$$= \lim_{x\to-\infty} \lim_{n\to\infty} \mathrm{e}^{-qx} \hat{u}_n(1+q) = 0 \tag{20}$$

so that $O^+ = 1$ in regime 1. Note that reversing the order of the limits in equation (19) so that

$$O^+ = \lim_{n\to\infty} \lim_{\epsilon\to+0} \int_0^\epsilon p_n(y)\,\mathrm{d}y$$

implies $O^+ = 0$ instead of 1. This situation has an analogy with more conventional order parameters. For example, consider a magnetic system given random spin flip

dynamics (as in a Monte Carlo simulation). Denote the brackets $\langle \ldots \rangle$ as the ensemble average over all random numbers employed. Suppose at time $t=0$, we start the spins in an unaligned configuration so that $\langle S(0)\rangle = 0$. The order parameter, O, represents the average magnetisation of a spin S in the ordered phase so that

$$O = \lim_{h\to+0}\lim_{t\to\infty}\langle s(t,h)\rangle = \lim_{h\to+0}\lim_{t\to\infty}\int_0^h \left\langle \frac{\mathrm{d}s(t,h')}{\mathrm{d}h'}\right\rangle \mathrm{d}h' \tag{21}$$

(where h is an applied field) which has a non-zero value. However, if we reverse the order of the limits then $O=0$. The similarity between the transitions in these maps and conventional statistical mechanics is similar to the interpretation of the effects of noise on the transition to chaos in the mapping used by Feigenbaum. The interpretation given by Huberman and Rudnick (1980) (also see Crutchfield *et al* 1981) is that the amplitude of the noise is analogous to the strength of an applied magnetic field near a phase transition. This is because noise has the effect of smearing out the period doubling sequence causing what they call a 'bifurcation gap'. In other words, adding noise to the Feigenbaum map stops the infinite cascade of bifurcation from occurring, which is similar to the effects of a magnetic field, in that a magnetic field also smears out the transition between the ordered and the disordered states. In the transitions discussed in this paper, however, the amplitude of the noise does not control the phase of the map. It is the derivative of the noise that is important as can be seen from the definition of the order parameter.

Now we discuss the case of non-zero $v(x)$. There are two cases to consider depending on whether the value of s that minimises $\hat{u}(s)+\hat{v}(s)$, denoted by s^*, is greater or less than 1. We call the case where $s^*>1$, regime 2, and the case $s^*<1$, regime 3 (see figure 1). Both $\hat{u}(s)$, $\hat{v}(s)>0$ so that $\hat{u}_n+\hat{v}_n(s)>\hat{u}_n(s)-\hat{v}_n(s)$ and by equation (10) $\hat{u}(1)+\hat{v}(1)=1$. This implies that in the neighbourhood of $s=1$, $\hat{u}(s)-\hat{v}(s)<1$. Equation (15*b*) implies that

$$\hat{u}_n(2)-\hat{v}_n(2) = \int_0^\infty xp(x)\,\mathrm{d}x + \int_{-\infty}^0 xp(x)\,\mathrm{d}x = 1. \tag{22}$$

This means that $\hat{u}_n(2)+\hat{v}_n(2)>1$ as illustrated in figure 1. So in regime 2, and for some sufficiently small $s>1$, one has that

$$\lim_{n\to\infty}\hat{u}_n(s) < \lim_{n\to\infty}(\hat{u}(s)+\hat{v}(s))^n = 0 \tag{23}$$

so that $u_n(s)=v_n(s)=0$.

We now define a new order parameter

$$O^- = \lim_{\varepsilon\to+0}\lim_{n\to\infty}\int_{-\varepsilon}^0 p_n(y)\,\mathrm{d}y \tag{24}$$

and observe that in regimes 2 and 3 that

$$\begin{aligned}\lim_{n\to\infty}\int_0^\infty u_n(x)\,\mathrm{d}x &= \lim_{n\to\infty}\hat{u}_n(1)=\tfrac{1}{2}\\ \lim_{n\to\infty}\int_0^\infty v_n(x)\,\mathrm{d}x &= \lim_{n\to\infty}\hat{v}_n(1)=\tfrac{1}{2}.\end{aligned} \tag{25}$$

Then, using arguments analogous to those used in regime 1, we have that for some

sufficiently small $q>0$

$$\begin{aligned}\tfrac{1}{2}-O^{+} &= \lim_{x\to-\infty}\lim_{n\to\infty}\int_{x}^{\infty} e^{y}u_n(y)\,dy \\ &\leqslant \lim_{x\to-\infty}\lim_{n\to\infty}\int_{-\infty}^{\infty} e^{y}u_n(y)\,e^{q(y-x)}\,dy \\ &= \lim_{x\to-\infty}\lim_{n\to\infty} e^{-qx}\hat{u}_n(1+q)=0 \end{aligned} \tag{26}$$

so that O^{+}, and similarly $O^{-}=\frac{1}{2}$ in regime 2. In regime 3 we define two parameters which we will see later represent 'disorder':

$$D^{\pm}=\pm\lim_{x\to\infty}\lim_{n\to\infty}\int_{\pm x}^{\pm\infty} p_n(w)\,dw. \tag{27}$$

Then it is straightforward to show that $D^{+}=D^{-}=\frac{1}{2}$ in regime 3.

In summary we have that in regime 1, $O^{+}=1$, $O^{-}=0$, $D^{+}=D^{-}=0$. As soon as we let $v(x)$ become non-zero, we enter regime 2 which means that there is a discontinuous change in order parameters to $O^{+}=O^{-}=\frac{1}{2}$ and $D^{+}=D^{-}=0$. Then as the variance of $p(x)$ is increased, there is another discontinuous jump whereupon $O^{+}=O^{-}=0$ and $D^{+}=D^{-}=\frac{1}{2}$.

To make the above remarks more transparent, we will consider some explicit forms for $p(w)$ that illustrate the three different regimes. First consider

$$p(w)=\begin{cases}0 & w<a \\ \dfrac{1}{2(1-a)} & a<w<2-a \\ 0 & w>2-a\end{cases} \tag{28}$$

where $0<a<1$. This satisfies the conditions of equation (15), and $g_n(x)$ should be in regime 1. So equation (14) gives $\hat{u}_n(s)=\hat{u}^n(s)$, so that for large n, $u_n(x)$ should be approximately Gaussian with a mean $x=\frac{1}{2}n[\ln(2-a)+\ln(a)]$, and a variance $\{\ln[(2-a)/a]\}^2 n/12$. As n goes to infinity x goes to infinity linearly whereas the width of the Gaussian increases as $n^{1/2}$. So $u_n(x)$ is compressed towards $x=0$ as n goes to infinity. If we define $I_n(x)=|\int_0^x p_n(x')\,dx'|$ then as n increases $I_n(x)$ also increases and approaches 1. This is because for any $x>0$, we find that for large enough n, $p_n(x)$ has compressed to fit almost completely inside the interval between 0 and x. $I_n(x)$ for regime 1 is illustrated in figure 2(a). The arrow denotes the direction the function shifts with increasing n.

Next we consider $p(w)$ in either regime 2 or 3:

$$p(w)=\begin{cases}0 & w<-a \\ 1/2b & -a<w<a \\ 1/b & a<w<b \\ 0\end{cases} \tag{29}$$

which satisfies equation (15a). Equation (15b) implies that $a=[(b-1)^2-1]^{1/2}$. Now we want to calculate $I_n(x)$ for $x>0$. We first observe that the second term in equation (14a) $(\hat{u}(s)-\hat{v}(s))^n$ gives negligible contribution to $I_n(x)$ for large n as was shown above. To calculate the contribution from $(\hat{u}(s)+\hat{v}(s))^n$, we take the inverse Laplace

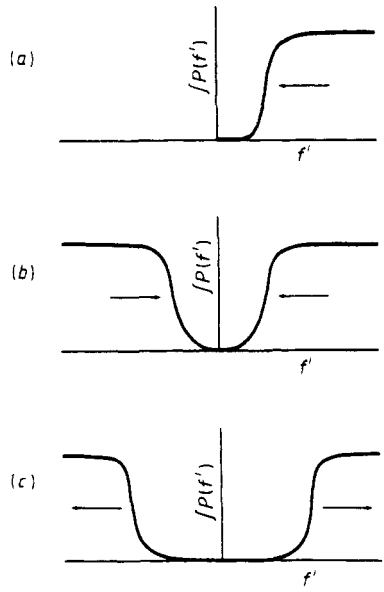

Figure 2. $I_n(f')$ plotted against f' in all three regimes where I_n is defined in the text. In (a) regime 1 is shown. As n increases, I_n is compressed towards the vertical axis. I_n is zero for $f'<0$. In (b) regime 2 is shown. As n increases, I_n becomes more symmetric but compressed towards the verticle axis. Regime 3 is shown in (c). As n increases, I_n expands, away from the vertical direction.

transform, i.e. for large n

$$\begin{aligned}\mathscr{L}^{-1}(\hat{u}_n(s)) &= \mathscr{L}^{-1}\left[\left(\frac{1}{b}\int_{-\infty}^{\ln b} e^{sy}\,dy\right)^n\right] \\ &= \frac{1}{b^n 2\pi i}\int_{-\infty}^{\infty}\frac{\exp[ik(x-n\ln b)]}{(ik)^n}\,dk \\ &= \frac{(n\ln b - y)^{n-1}}{b^n(n-1)!}\end{aligned} \tag{30}$$

for $y < n \ln b$. Therefore

$$p_n(x) = \frac{(\ln x/b^n)^{n-1}}{b^n(n-1)!}$$

for $x < b^n$. $I_n(x)$ for large n becomes

$$I_n(x) = \int_{-\infty}^{\ln x}\frac{e^y(n\ln b - y)^{n-1}}{b^n(n-1)!}\,dy. \tag{31}$$

The maximum in this integrand occurs at $y = 1 + n\ln(b/e)$. When $b < e$, the maximum of the integrand moves linearly with n in the negative y direction, as in the first example, and so $O^+ = O^- = \frac{1}{2}$. However, for $b > e$, the maximum of the integrand moves linearly with n in the positive y direction so that $O^+ = O^- = 0$ and $D^+ = D^- = \frac{1}{2}$. $I_n(x)$ is illustrated in figures 2(b) and 2(c) in regimes 2 and 3, respectively.

Using these results, the behaviour of the function $g_n(x)$ for large n can now be discussed in the three separate regimes. In regime 1, $g_n(x)$ must be monotonic, i.e. $g'_n(x) > 0$, and since $O^+ = 1$, the probability as n tends to infinity, that the slope is zero at any arbitrary point, is unity. Therefore the function consists of random 'steps' of average width and separation proportional to $n^{1/2}$, since by equation (5) $\langle (g_n(x) - x)^2 \rangle$ is proportional to n. The slope of the steps increases exponentially since $\langle g'^2_n(x) \rangle = \langle (f'(x))^2 \rangle^n$ increases exponentially with n. As n is increased, adjacent steps randomly shift position until they 'collide' forming a larger step. In regime 2

$$\langle |g'_n(x)| \rangle = \langle |f'_n(g_{n-1}(x)) g'_{n-1}(x)| \rangle = \langle |f'(x)| \rangle^n \tag{32}$$

which diverges exponentially. This represents the average length of path $g_n(x)$ traces out, projected onto the direction of the y axis. Since $O^+ = O^- = \frac{1}{2}$ then as in regime 1, as n tends to infinity, the probability that the slope is zero at any arbitrary point, is unity, which implies that in this regime there are either a large number of 'kinks', i.e. portions of the curve with a large ratio of height to width, or a large number of downwards steps, or both kinks and downwards steps. We will see in § 4 that if we iterate a function consisting of upwards and downwards steps of finite width, then the number of downwards steps per unit length goes to zero. Therefore as n goes to infinity the number of kinks increases exponentially while the total fraction of the x axis occupied by kinks goes to zero. In regime 3, and as n goes to infinity, the total fraction of the x axis occupied by kinks goes to 1. This means that the function oscillates on very small length scales, the average frequency of oscillation diverging exponentially with n. These remarks will be confirmed in § 5 when we discuss the numerical implementation of the maps.

4. The discretised model

To further elucidate the nature of these transitions, and to give a natural physical interpretation of these mappings, the analogous problem described by equations (1) and (2) was studied on the integers. The variable x is now defined on the integers, as is the noise $\varepsilon(x)$. This discretisation eliminates the high frequency components of $g_n(x)$ that occur in regimes 2 and 3.

The physical interpretation of this map is as follows. Consider particles on a one-dimensional lattice. Each iteration of the map corresponds to evolution of the particles' motion to the next time step. At time $t = 0$ the ith site contains a particle labelled i. At time $t = 1$, site $f_1(i)$ contains the ith particle, so that particle i has hopped a distance $\varepsilon_1(i)$ in the first time step. Site $f_1(i)$ may contain more than one particle, i.e. if $f_1(i) = f_1(j)$ then site $f_1(i)$ contains both particles i and j. This situation is illustrated by an example for six particles in figure 3. The transformation plotted in (a) interchanges particles 1 and 2, and 5 and 6. It maps both particles 3 and 4 into site 4, leaving site 3 vacant. At $t = 2$, the next iteration transforms the position of the ith particle from $f_1(i)$ to $f_2(f_1(i))$. For $t = n$, the value of i labels each individual particle, and the value of $g_n(i)$ labels the position along the lattice. As a consequence of these dynamics, two particles occupying the same site will move together in all subsequent time steps. Thus the discretised version of equations (2) and (3) describes a problem of aggregation where the diffusion coefficients of the aggregates are all equal.

With this physical interpretation of the discretised maps, we see that the probability of particle i being at site j after n steps is $P_n(i; j)$ as is given by equation (6). As in

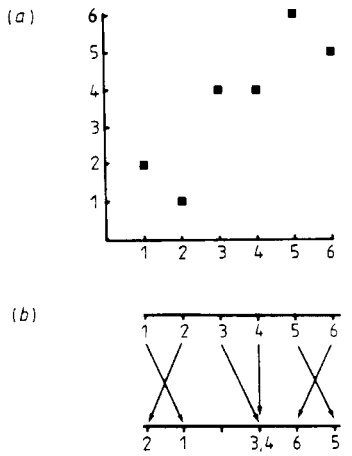

Figure 3. (*a*) An example of a random iteration $f_1(x)$ restricted to the integers and (*b*) its corresponding interpretation as the dynamics for aggregating particles (see the text for a full explanation).

the continuous case, equation (6) shows no change in analytic structure as the hopping probabilities between sites, $P(\varepsilon)$, are varied. In the discretised model, it is not possible to define a probability distribution for the derivatives of g_n. Therefore in order to compare the behaviour of the continuous case with the discretised problem, we consider the probability that $g_n(x_2)-g_n(x_1)=a$ after n time steps, which we call $p_n(a; x_2-x_1)$. Then

$$\begin{aligned} p_n(a;\Delta x) &= \langle \delta(g_n(x+\Delta x)-g_n(x)-a)\rangle \\ &= \langle \delta(g_{n-1}(f_1(x+\Delta x))-g_{n-1}(f_1(x))-a\rangle \\ &= \int \mathrm{d}y\, \langle \delta(f_1(x+\Delta x)-f_1(x)-y)\rangle p_{n-1}(a;y) \\ &\equiv \int \mathrm{d}y\, p_1(y;\Delta x)p_{n-1}(a;y). \end{aligned} \tag{33}$$

The discretised version of equation (33) is the probability that $g_n(j)-g_n(i)=a$, $p_n(a; j-i)$ and similarly

$$p_n(a;j)=\sum_k p_{n-1}(a;k)p_1(k;j). \tag{34}$$

Now we concentrate on the case where the correlations in $\varepsilon(x)$ are local. This corresponds to the forces between the aggregates being short ranged. In particular, we look at the case where each aggregate hops independently until it hits another aggregate. We want to determine the form of $p_1(k;j)$, and to do so, consider the probability $Q(m;l)$ that a function $f_1(l)$ equals m. Then because of translational invariance (equation (3)), $Q(m;l)\equiv Q(m-l)$. So for $j\neq 0$

$$\begin{aligned} p_1(k;j) &= \sum_{m,n} Q(m-l-j)Q(n-l)\delta_{m-n,k} \\ &= \sum_n Q(n+k-j)Q(n) \equiv p(k-j) \end{aligned} \tag{35}$$

where $p(k)$ is the probability that two particles on different sites, will have changed in relative position by a distance k in one time step and since the function $f(j)$ is single valued, for $j = 0$

$$p_1(k;0) = \delta_{k,0} \tag{36}$$

so $p_1(k;j)$ can be expressed in the form

$$p_1(k,j) = p(k-j) + \delta_{j,0}(\delta_{k,0} - p(k)). \tag{37}$$

Laplace transforming $p_n(a;j)$ with respect to n, and decomposing j into its Fourier components defines $P_s(a, q)$ as

$$P_s(a, q) = \int_0^\infty \sum_j e^{-ns}\, e^{iqj} p_n(a;j)\, dn. \tag{38}$$

So equation (34) becomes

$$e^s P_s(a, q) - e^{iaq}\frac{(e^s-1)}{s} = P_s(a;q)p(q) + \frac{1}{2\pi}\int_{-\pi}^{\pi} P_s(a;q)(1-p(q))\, dq. \tag{39}$$

The second term in this equation expresses the initial condition that $p_0(a;j) = \delta_{a,j}$. After some tedious algebra this can be solved to give

$$P_s(a;q) = \frac{(e^s-1)}{s}\frac{e^{iaq}}{e^s - p(q)} + \frac{2\pi}{s}\delta_{a,0} - \left(\frac{(e^s-1)}{s}\int_{-\pi}^{\pi}\frac{e^{iq'a}}{e^s - p(q')}\, dq'\right) \times\left((e^s - p(q))\int_{-\pi}^{\pi}\frac{dq'}{e^s - p(q')}\right)^{-1}. \tag{40}$$

For $a = 0$ this can be simplified further to give

$$P_s(0;q) = \frac{2\pi}{s(e^s - p(q))}\left(\int_{-\pi}^{\pi}\frac{dq'}{e^s - p(q')}\right)^{-1}. \tag{41}$$

The inverse Laplace and Fourier transform of $P_s(a, q)$ is

$$p_n(a;j) = \frac{1}{2\pi i}\int_{-i\infty+c}^{i\infty+c}\frac{1}{2\pi}\int_{-\pi}^{\pi} P_s(a, q)\, e^{iqj}\, dq\, e^{ns}\, ds. \tag{42}$$

To obtain $p_n(a;q)$, we will consider a specific form for $p(j)$. The results apply qualitatively to the general case. We take $Q(l)$ to be

$$Q(l) \equiv (1-A)\delta_{l,0} + \tfrac{1}{2}A(\delta_{l,-1} + \delta_{l,1}) \tag{43}$$

where A is a parameter. This means that in one time step the probability of an aggregate remaining at the same site is $1 - A$, and the probability of moving to an adjacent site is A.

The detailed calculation of $p_n(0;1)$ is relegated to the appendix. To leading order in $1/n$ the result is

$$p_n(0;1) \doteq 1 - \frac{1}{2}\frac{1}{[A(1-A)]^{1/2}}\frac{1}{(\pi n)^{1/2}}. \tag{44}$$

So for A not equal to 0 or 1, aggregation occurs and the behaviour of g_n is similar to that of regime 1 in the continuous case. For $A = 1$, aggregation cannot occur between adjacent sites. Odd numbered sites aggregate with each other as do even numbered

sites (i.e. $p_n(0;1)=0$). This behaviour is similar to regime 3 of the continuous case, but only occurs for $A=1$, instead of being present over a continuous range of parameters.

5. Numerical calculations

To investigate the map numerically, the simplest algorithm would be the following. A finite interval, from 1 to N, is chosen. At every integer i in this interval a random number $\varepsilon(i)$ is generated of variable amplitude. We take the random numbers to be evenly distributed from $-a$ to a. The three different regimes can be investigated by varying the value of a. The function in equation (2) can then be calculated on the integers. To obtain the value of $f_n(x)$ for an arbitrary real number on this interval we take $f_n(x)$ to vary linearly between the integers, i.e.

$$f_n(x)=f_n(\text{int}(x))+(x-\text{int}(x))(f_n(\text{int}(x)+1)-f_n(\text{int}(x))) \tag{45}$$

where $\text{int}(x)$ stands for the largest integer less than x. So $g_n(x)$ can be computed from $g_{n-1}(i)$ by setting $x=g_{n-1}(i)$ in equation (45). The only numbers that have to be stored at the nth iteration are $g_{n-1}(i)$ and $f_n(i)$, for $i=1$ to N.

There are problems with such an algorithm in all three regimes. In regime 1, the slope at an 'edge' is not properly determined as $g_n(x)$ is only sampled at finite intervals, and so the behaviour in this regime cannot be completely verified. In the preceding section it was established that as n tends to infinity, the proportion of the x axis occupied by kinks goes to zero, hence the probability of sampling a kink goes to zero for large n. Therefore regime 2 will appear to behave the same way as regime 1, i.e. $g_n(x)$ will have the form of ascending steps for large n. In regime 3, the iterated function should oscillate at arbitrarily high spatial frequency as n tends to infinity, but because the function is only probed at finite intervals, it will look as if the average frequency of oscillation is approaching a constant, namely the inverse of the distance between adjacent sampling points.

One might try and eliminate the above difficulties by sampling the points at equal intervals but very close together compared to the variations in $f_n(x)$. However the arguments in the last paragraph point out that this will not be satisfactory. In other words, although $f_n(x)$ is a continuous function, the iterated function $g_n(x)$ approaches a discontinuous function in all three regimes as n goes to infinity, so even sampling of points does not give satisfactory results. These remarks were verified by implementing the above algorithm on a computer.

An improvement on this method is to sample points at variable intervals that depend on the value of the iterated function, so that all portions of the iterated function are probed. We label the points being sampled in the $(n-1)$th iteration $x_{n-1}(i)$ where i takes the values 1 to m, and m, which is the total number of points being sampled in iteration $n-1$, will in general increase with additional iterations. The algorithm employed is such that the points $x_{n-1}(i)$ sample all the minima and maxima of $g_{n-1}(x)$. To see how this is done, we proceed by inductive reasoning and first examine the procedure by which the points $x_n(i)$ are generated.

The points $x_{n-1}(i)$ have the natural ordering

$$x_{n-1}(1)<x_{n-1}(2)<\ldots<x_{n-1}(m) \tag{46}$$

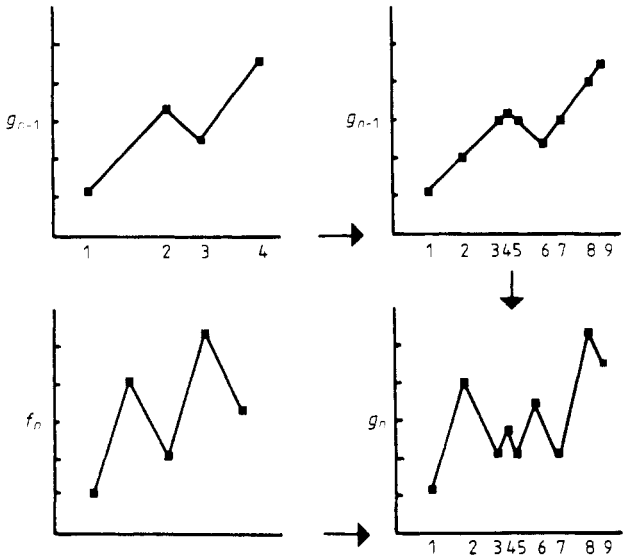

Figure 4. Illustration of the construction of iterated functions using the method described in the text. The upper left-hand graph shows $g_{n-1}(x)$. The numbers on the horizontal axis label the positions of $x_{n-1}(i)$. In the upper right-hand graph, additional points have been marked where $g_{n-1}(x)$ has integer values. All the marked points correspond to x coordinates labelled $x(1), \ldots, x(9)$. The lower left-hand graph shows the function $f_n(x)$ which changes slope only at the integers. Finally $f_n(g_{n-1}(x))$ is shown. The points $x_n(i)$ allow one to correctly compute all the maxima and minima since the function $f_n(x)$ varies linearly between the integers. Hence this method gives an exact reproduction of $g_n(x)$ for all x.

as displayed in the upper left-hand graph of figure 4, where the numbers on the horizontal axis represent the subscript i. Between an interval $\{x_{n-1}(i), x_{n-1}(i+1)\}$ the following procedure is implemented. All values of x inside this interval with the property that $g_{n-1}(x)$ is an integer are generated. This is easily done since the function $g_{n-1}(x)$ is linear on this interval. This is because we are taking $f_n(x)$ to be of the form given in equation (45), so the iterated function $g_{n-1}(x)$ must be composed of linear sections (this is explained in more detail below). These values of x (that correspond to $g_{n-1}(x)$ being integer valued) are then stored for the intervals

$$\{x_{n-1}(i), x_{n-1}(i+1)\} \tag{47}$$

in addition to the coordinates $x_{n-1}(i)$. All of these coordinates are then renumbered according to inequality (46) and are stored as the array $x_n(i)$ (see the upper right-hand graph of figure 4). The iterated function $g_n(x)$ is generated from the array $x_n(i)$ by computing $f_n(g_{n-1}(x_n(i)))$ (see the bottom two graphs in figure 4). Note that between $x_n(i)$ and $x_n(i+1)$, $g_n(x)$ is linear since the interval $\{g_{n-1}(x_n(i)), g_{n-1}(x_n(i+1))\}$ can only contain an integer value at its beginning $(g_{n-1}(x_n(i)))$ or its end $(g_{n-1}(x_n(i+1)))$, so the function $f_n(x)$ is linear on this interval and therefore so is $g_n(x)$. So we can proceed to the next iteration by applying the same procedure as above to the array $x_n(i)$ to obtain the array $x_n(i+1)$, and so on.

Some illustrations of functions generated with the above algorithms are shown in figures 5-7, showing the iterated functions in all three regimes.

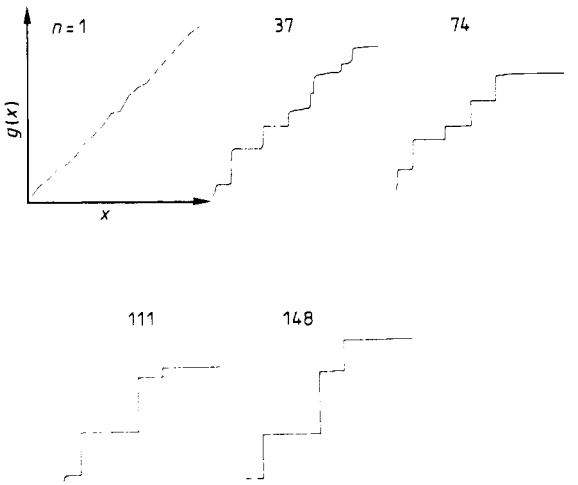

Figure 5. A sequence of 148 iterations of the map shown in steps of 37, using the algorithm shown in figure 5. In this case $a = 0.45$ so the functions $f_i(x)$ are monotonic, and so $g_n(x)$ is in regime 1. 20 random points are selected on each iteration according to equation (45), i.e. x ranges from 1 to 20.

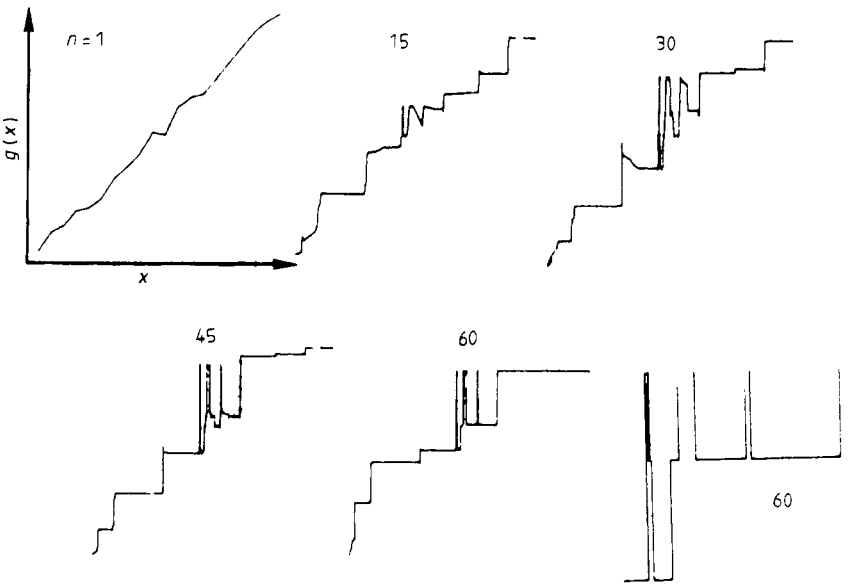

Figure 6. A sequence of 60 iterations of a map with $a = 0.75$, shown in steps of 15. Again the values of x range from 1 to 20. It is clear from the behaviour of the iterated function that is in regime 2. The last frame (lower right-hand corner) shows part of the function on the 60th iteration blown up to illustrate the kinks that are generated in regime 2.

6. Conclusions

In conclusion, we have shown the existence of a new type of transition induced by noise that occurs in iterative maps. The transition between regimes 2 and 3 are

Figure 7. $f_1(x)$ and $g_6(x)$ with $a = 3.0$. The interval along the x axis is between 1 and 20. The last frame (right-hand side) is a blown-up section of $g_6(x)$, showing the peculiar high frequency structure characteristic of regime 3.

reminiscent of the onset of turbulence, in that an instability forms whereby some wavelength fluctuations become unstable. The analogy can be made more specific by considering a fluid at time t and at some later time, $t+T$. There is a transformation that maps all the points in fluid at time t to all points at time $t+T$. In general, this map will depend on the complete velocity distribution of all the points. If we make the crude simplification that the transformation shifts points in space by random amounts (which might mimic the nonlinearity of the equations of motion), then we arrive at the three-dimensional version of equation (1). To prevent 'aggregation' of points in space as occurs in the one-dimensional case, we can require that the Jacobian of the transformation at every point equal 1, which makes the fluid incompressible. It has also been shown (Deutsch 1985) that these maps are closely related to the behaviour of non-interacting particles in one dimension, with inertia in a viscous media subject to a random force $f(x, t)$. The random force is correlated only locally in space and time as

$$\langle f(x, t)f(x', t')\rangle = g(x - x')\delta(t - t') \tag{48}$$

where $g(x)$ is a rapidly decaying function with a parabolic maximum at $x = 0$. The equation of motion of a single particle in such an environment is

$$m\ddot{x} + \nu\dot{x} = f(x, t) \tag{49}$$

where m is the mass of an individual particle and ν is the friction coefficient. If we consider the motion of this particle on its own, then for long times $\langle x^2\rangle \propto t$ (in analogy with equation (6)). Now consider many particles that are equally spaced at $t = 0$ all obeying (49). When m is below some critical value that depends on $g(x)$ and ν, the particles aggregate. Particles come together forming aggregates, these aggregates come together forming still larger aggregates, and so on. The analogy with the maps considered in this paper can be made more specific if we plot the final position of particles as a function of their initial condition. As time progresses, the function develops sharp steps similar to what is obtained in regimes 1 and 2 of the maps. The pieces of the function having nearly zero slope represent aggregates. The number of iterations of the map is analogous with the time parameter in (49). When m is above the critical value mentioned above, particles cease to aggregate, and one obtains behaviour similar to regime 3 of the random maps considered in this paper.

Acknowledgments

The author is indebted to Professor S F Edwards, Dr R C Ball, Dr R Joynt, Dr S Marianer and B O'Shaughnessy for useful discussions.

Appendix

In this appendix, the detailed derivation of (44) is presented. By (35)

$$p(q)=\frac{A^2}{2}+(1-A)^2+2A(1-A)\cos q+\frac{A^2}{4}\cos 2q. \tag{A1}$$

If the integral in equation (42) over q is performed first, we are left with an integral in the complex s plane. The integrand has a set of branch cuts parallel to the real axis. The values which determine the locus of the branch cuts, s_b, are given by the condition that for some $-\pi<q<\pi$

$$e^{s_b}=p(q) \tag{A2}$$

since the integrand picks up an imaginary part and is therefore discontinuous between the points $s_b+i\varepsilon$ and $s_b-i\varepsilon$. It is clear that the branch cuts all end where $\mathrm{Re}(s)=0$, since the maximum value of $p(q)$ is at $p(0)$ and equals 1. If $p(q)>0$ for all $-\pi<q<\pi$ then the branch cut will start at $s=\ln(p_{\min})+2\pi n i$, with n being any integer and $p_{\min}$ being the minimum value of $p(q)$, and the cut ends at $s=2\pi n i$. If $p_{\min}<0$ there will be an additional set of branch cuts starting at $s=\ln p_{\min}+(2n+1)\pi i$ and ending at $(2n+1)\pi i$. In the case of interest, however, $p(q)>0$ for all A. Now we calculate the integral over q explicitly in equations (41) and (42) by making the substitution $z=e^{iq}$ so

$$\begin{aligned}F(a,s)&=\int_{-\pi}^{\pi}\frac{e^{iqa}}{e^s-p(q)}\\&=\oint_c\frac{z^a\,dz/iz}{e^s-[A^2+(1-A)^2+A(1-A)(z+1/z)+\frac{1}{4}A^2(z^2+1/z^2)]}\end{aligned} \tag{A3}$$

the contour being the circle $z=1$. We have labelled this integral $F(a,s)$ for convenience. There are four poles in the integrand, at z_1, z_2 and by symmetry two others at $1/z_1$ and $1/z_2$. The quartic equation for the poles can therefore be reduced to two quadratic equations giving the poles at

$$\begin{aligned}z_1&=\left(1-\frac{1}{A}+\frac{e^{s/2}}{A}\right)-\left[\left(1-\frac{1}{A}+\frac{e^{s/2}}{A}\right)^2-1\right]^{1/2}\\z_2&=\left(1-\frac{1}{A}-\frac{e^{s/2}}{A}\right)+\left[\left(1-\frac{1}{A}-\frac{e^{s/2}}{A}\right)^2-1\right]^{1/2}\\z_1^{-1}&=\left(1-\frac{1}{A}+\frac{e^{s/2}}{A}\right)+\left[\left(1-\frac{1}{A}+\frac{e^{s/2}}{A}\right)^2-1\right]^{1/2}\\z_2^{-1}&=\left(1-\frac{1}{A}-\frac{e^{s/2}}{A}\right)-\left[\left(1-\frac{1}{A}-\frac{e^{s/2}}{A}\right)^2-1\right]^{1/2}.\end{aligned} \tag{A4}$$

The large n behaviour of $p(a;n)$ is determined by the region $0>\mathrm{Re}(s)\gg -1$, so we

are interested in the value of $F(a, s)$ in this regime. The contour in the complex s plane is shown in figure A1. Then $|z_2| > 1 > |1/z_2|$. For s lying on the branch cut, the square root in equation (A4) is pure imaginary so that $z_1 = 1/z_1 = 1$. If we displace s slightly above the branch cut, i.e. let $s^+ = s_b + i\varepsilon$ with $\varepsilon > 0$, then $|z_1| < 1 < |1/z_1|$. So above the branch cut the poles that contribute the $F(a, s^+)$ are z_1 and z_2. Below the branch cut at $s^- = s_b - i\varepsilon$, the poles that contribute to $F(a, s^-)$ are $1/z_1$ and z_2. Thus

$$F(a, s^+) = -\frac{1}{2\pi}\left(\frac{z_1^{a+1}}{(z_1 - 1/z_1)(z_1 - z_2)(z_1 - 1/z_2)} + \frac{z_2^{a+1}}{(z_2 - 1/z_2)(z_2 - 1/z_1)(z_2 - z_1)}\right) \tag{A5}$$

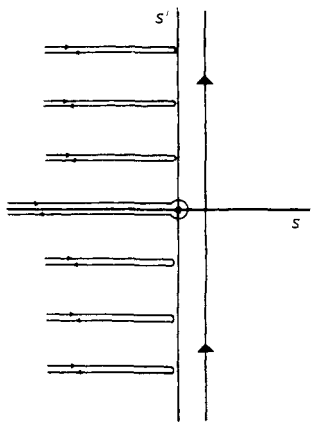

Figure A1. The contour chosen in evaluating the integral in equation (42) shown in the complex s plane. The solid circle at the origin represents a first-order pole. The path of integration is taken around all branch cuts.

and

$$F(a, s^-) = \frac{-1}{2\pi}\left(\frac{z_2/(z_1)^a}{[(1/z_1) - z_1][(1/z_1) - z_2](z_2 - z_1)} + \frac{z_2^{a+1}}{(z_2 - 1/z_2)[(1/z_2) - (1/z_1)](z_2 - z_1)}\right). \tag{A6}$$

Expressing equation (42) in terms of $F(j, s)$

$$p_n(0; j) = \frac{1}{2\pi i}\int_{-i\infty+c}^{i\infty+c} \frac{e^{ns}}{s}\frac{F(j, s)}{F(0, s)}\,ds \tag{A7}$$

implies that we have to calculate the value of $F(j, s)/F(0, s)$ as $s \to 0$ in order to calculate the contribution from the pole at $s = 0$. Now

$$\frac{F(j, s^+)}{F(0, s^+)} = \left(\frac{z_1^j}{z_1 - 1/z_1} - \frac{z_2^j}{z_2 - 1/z_2}\right)\left(\frac{1}{z_1 - 1/z_1} - \frac{1}{z_2 - 1/z_2}\right)^{-1} \tag{A8}$$

and

$$\frac{F(j, s^-)}{F(0, s^-)} = \left(\frac{1/z_1^j}{z_1 - 1/z_1} + \frac{z_2^j}{z_2 - 1/z_2}\right)\left(\frac{1}{z_1 - 1/z_1} + \frac{1}{z_2 - 1/z_2}\right)^{-1} \tag{A9}$$

both of which go to 1 as $s \to 0$, since $z_1 - 1/z_1 = 0$ at $s = 0$. The pole at $s = 0$ therefore gives a total contribution of 1 to $p_n(0; j)$.

Now we calculate the contribution from the cut at $\mathrm{Im}(s) = 0$. If we subtract the upper from the lower contour we obtain

$$\frac{F(j, s^+)}{F(0, s^+)} - \frac{F(j, s^-)}{F(0, s^-)} = \left(z_1 - \frac{1}{z_1}\right)\left(1 + \frac{z_1 + (1/z_1) - 2z_2}{z_2 - 1/z_2}\right)\left[1 - \left(\frac{z_1 - 1/z_1}{z_2 - 1/z_2}\right)^2\right]^{-1}. \tag{A10}$$

In the limit $-1 \ll s < 0$ this reduces to

$$\left(z_1 - \frac{1}{z_1}\right)\frac{1}{(1-A)^{1/2}} = \frac{s^{1/2}}{[A(1-A)]^{1/2}} \tag{A11}$$

so the integrand along this branch cut behaves as $s^{-1/2}$ for small s. To obtain the large n behaviour, we extract the contributions from the lowest order terms in $\mathrm{Re}(s)$. We have isolated two terms: the first proportional to s^{-1} which comes from the pole at $s = 0$, and the second proportional to $s^{-1/2}$ which comes from the branch cut at $\mathrm{Im}(s) = 0$. It is easy to see that the contribution from all other branch cuts is of lower order in $\mathrm{Re}(s)$ since if we parametrise s along a branch cut as $s = 2\pi n\mathrm{i} + x$ then this contribution to $p(0; 1)$ is proportional to

$$\begin{aligned}
&\int_{-\infty}^{0} \mathrm{d}x\, \mathrm{e}^{nx} \sum_{\substack{n' \neq 0 \\ n=-\infty}}^{\infty} \frac{x^{1/2}}{2\pi\mathrm{i}n' + x} \\
&\quad = \int_{-\infty}^{\infty} \mathrm{d}x\, \mathrm{e}^{nx} \sum_{n'>0} \frac{x^{1/2} 2x}{n'^2 + x^2} \\
&\quad \leqslant \int_{-\infty}^{0} \mathrm{d}x\, \mathrm{e}^{nx} \int_0^{\infty} \frac{x^{1/2} 2x}{4\pi^2 n^2 + x^2}\, \mathrm{d}n \propto \int_{-\infty}^{0} \mathrm{d}x\, x^{1/2}\, \mathrm{e}^{nx}.
\end{aligned} \tag{A12}$$

So to leading order in $1/n$

$$\begin{aligned}
p_n(0; 1) &= 1 - \int_0^{\infty} \frac{\mathrm{e}^{-nx}}{2\pi x^{1/2}[A(1-A)]^{1/2}}\, \mathrm{d}x \\
&= 1 - \int_0^{\infty} \frac{\mathrm{e}^{-ny^2}}{\pi[A(1-A)]^{1/2}} = 1 - \frac{1}{2}\frac{1}{[A(1-A)]^{1/2}}\frac{1}{(\pi n)^{1/2}}.
\end{aligned} \tag{A13}$$

References

Crutchfield J, Nauenberg M and Rudnick J 1981 *Phys. Rev. Lett.* **46** 933-5

Deutsch J M 1984 *Phys. Rev. Lett.* **52** 1230-3

—— 1985 *J. Phys. A: Math. Gen.* **18** 1449-56

Feigenbaum M J 1978 *J. Stat. Phys.* **19** 25

Geisel T and Nierwetberg J 1982 *Phys. Rev. Lett.* **48** 7-10

Feigenbaum M J and Hasslacher B 1982 *Phys. Rev. Lett.* **49** 605-9

Hirsch J E, Huberman B A and Scalapino D J 1982 *Phys. Rev.* A **25** 519-32

Huberman B A and Rudnick J 1980 *Phys. Rev. Lett.* **45** 154-6

Shraiman B, Wayne C E and Martin P 1981 *Phys. Rev. Lett.* **46** 935-8